Induced AVO anomalies from pore pressure effects

Antonio C. Buginga Ramos and Marco A.S. Toledo, PETROBRAS S/A

Abstract

AVO anomalies are normally associated to changes in the rock's compressibility and density, which are normally caused by changes in lithology and saturant fluids. Frequently, however, AVO signatures can be quite ambiguous causing the need for well/seismic calibration using rock properties and reflectivity modeling. An important source of ambiguity is the abrupt drop in effective pressure, which affects the skeleton bulk moduli of the rock. Effective pressure is defined as the difference between the overburden pressure and the pore pressure. In clastic basins pore pressure largely controls the changes in seismic velocities. The primary cause of abnormal pore pressure is the disequilibrium compaction of shale, which is caused by subcompaction dewatering. Because water tend to be adsorbed on the clay particles, pore pressure has a much greater influence in the elastic properties of shales than it has in sands. In this paper, we show how the elastic properties of the shale cap rock can be affected by pore pressure causing significant changes in the AVO attributes. The change in elastic properties of the shale section can even induce false AVO anomalies, entirely related to the overpressure phenomenon. AVO pitfalls are particularly important in the contact between overpressured shales and high impedance sands.

Introduction

In recent years several authors have called the attention to the problem of pore pressure influence on rock property and the corresponding effect on seismic attributes and reflectivity modeling. Lindsay and Towner (2001) have shown the importance integrating 3D pore pressure volume in the seismic interpretation, in special using the seismically derived pressure data to predict the elastic properties for a prospect location under the influence of pore pressure. In their case, the elastic properties of a known well location were perturbed to include the effect of pore pressure. As result of their reflectivity modeling it was found that a strong negative AVO anomaly (amplitude decrease with offset) should be expected for hydrocarbon filled sands in the prospect location. Therefore, pore pressure effects in the shale cap rock have changed an otherwise positive AVO anomaly into a negative AVO, even in the presence of hydrocarbons. It is apparent from this example that pore pressure needs to be included in the AVO modeling design.

Carcione and Gangi (2000) have set out the mathematical basis for the effects of gas generation and overpressure on the seismic attributes. In their work the seismic velocities versus pore pressure and differential pressure are computed using a model for wave propagation in a porous medium saturated with oil and gas. In this work, we have looked in detail to changes in rock properties and AVO behavior below a known overpressure surface. The changes in the elastic properties of the overpressured shales have induced strong AVO anomalies which are not related to the presence of hydrocarbons. Particularly important is the fact the pore pressure changes the expected decrease of Poisson's ratio with depth for shales. Because shear velocity decreases more than compressional velocity as pore pressure increases, the net result is an increase in Poisson's ratio of the shales. Therefore, the knowledge of the abnormal pore pressure zone is fundamental to establish the limits of abnormal Poisson's ratio changes. These changes can cause abnormal values of AVO gradient, which in turn can produce false anomalies.

Methodology and Examples

Seismic velocities have been used to predict pore pressure using mainly models based on empirical relations. Our approach is based on quantifying the effects of abnormal pore pressure using control wells and subsequently using the expected change in rock properties for AVO modeling. Removal of the undesired effects of abnormal pore pressure from the expected rock property trends at a prospect location can substantially improve AVO modeling reducing the risk of drilling false anomalies.

Recognition of the false AVO anomalies is one of the critical aspects that this paper addresses. Many of these induced anomalies can have seismic behavior very close to those caused by hydrocarbon reservoirs embedded in normally pressured shales. To verify the unusual AVO behavior, a well drilled in a known overpressured area will be used as an example. Figure 1 shows the P-wave velocity, density, S-wave velocity and Poisson's ratio logs for the selected well. In terms of lithology this area is characterized by a typical binary clastic system (shales and sands). The shallow low impedance sands show typical class III AVO response, while the shallow high impedance sand shows a class II response. In the deeper section of the logs, high impedance sands are encased in low impedance shales. These shales are overpressured and show anomalously high Poisson's ratio (around to 0.41) and consequently anomalous Vp/Vs ratio (around 2.5) as indicated in Figure 2. The top of the overpressured zone is around 5000 m as indicated in Figures 2 and 3. This top represents the lower limit of the hydrocabon saturated sands. It also marks the limit of the AVO anomalies under influence of high porosity sands

filled by hydrocarbon saturants. A considerable contrast in Poisson's ratio is observed between the overpressured shales and the underlying high impedance sands, causing a relatively large and positive zero offset reflection coefficient, with a consequent large and positive AVO intercept. The contrast in Poisson's ratio between the high impedance sands and the overpressured shales is in the order of -0.18 (=0.23-0.41), causing a large and negative AVO gradient.

In order to make quantitative estimates of the strength of the AVO anomalies, we measured the orthogonal deviation from the background trend (fluid line) in the crossplots of AVO intercept versus gradient for each significant interface of the well. These interfaces correspond to shale/sand and sand/shale changes that appeared after blocking all logs with respect to the gamma-ray log. The values of orthogonal deviation for each interface were then normalized with respect to the overall standard deviation of these values. This procedure makes the measurements more quantitative and better correlated with similar seismic computations. Figure 4 shows the hydrocarbon and non-hydrocarbon induced AVO anomalies in terms of orthogonal deviation from the background trend. The hydrocarbon related anomalies are typically low impedance (class III) and high impedance (class II) sands embedded in normally pressured shales. The non-hydrocarbon anomalies are mainly negative orthogonal deviations (class I and II), which result from positive AVO intercepts and the strong negative AVO gradients.

Results

As stated earlier the effect of overpressure in the shale section is to cause a significant increase in the Poisson's ratio. In the example shown here, the overpressured shales have also low impedance when compared to the sands at same depth range. Therefore, the major contrasts of elastic parameters expected are: (a) for overpressured shale over brine sand: increase in impedance and drop in Poisson's ratio; (b) for brine sands over overpressured shales: decrease in impedance and increase in Poisson's ratio. These combinations of contrasts can create amplitude decrease with offset are typically found in class I and class II sands. The change in Poisson's ratio affects the AVO gradient causing deviations from background trend that can be stronger than those found in class II sands in the normal pressured section. Table 1 summarizes some elastic properties typically found in shales and sands located in the normal pressured and overpressured zones.

	Vp (m/s)	Vs (m/s)	Density (g/cm^3)	Poisson's Ratio	Background Deviation
Shale (normal)	2680	1200	2,41	0,37	-0,17
Oil Sand	3260	1940	2,22	0,22	
Shale (overp.)	2630	1034	2,36	0,41	-0,20
Brine Sand	3620	2150	2,36	0,23	

Table 1 – Elastic properties found in sands and shales in normal pressured and overpressured sections

Closer analysis of the overpressured zone in the standpoint of AVO analysis is found in Figures 5 and 6. In Figure 5, a synthetic CMP gather is shown, highlighting shales and sands found in the overpressured section. Horizons 1 to 4 indicated in the figure were selected for detailed analysis. Figure 6 shows the P-wave reflection coefficient responses for horizons 1 to 4. It is clear in the figure that horizons 1 and 3 correspond respectively to class I and class II anomalies, which are not related to pay.

Figure 7 shows the AVO crossplot for the depth interval that includes the HC-bearing high impedance class II sands (dotted squares) and also the water bearing class I and class II sands found in the overpressured section (solid circle). Without the knowledge of pore pressure effects these anomalies could easily be confused with pay zones.

Figure 8 shows the P-wave reflection coefficients for near (normal incidence) and far (30 degrees incidence) stacks as a function of effective pressure for sand/shale and shale/sand interfaces. The non-hydrocarbon related anomalies are indicated by a solid rectangle in the lower part of the figure. Polarity changes indicate class II AVO responses. A number of significant class II and class I AVO anomalies occur inside the selected zone. Despite the strength (Figure 4) these anomalies are all associated to contrasts between shales and water bearing sands.

Conclusions

It was demonstrated that class II and class I AVO anomalies can be induced and magnified by the effect of overpressure. These anomalies are false AVO responses since they may well correspond to contrasts between overpressure shale over brine sands and vice-versa. Consequently, the knowledge of the onset of overpressure is a very important piece of information for interpretation of AVO anomalies in shale/sand sequences. Fluid substitution modeling have shown that only a significant reduction in bulk modulus sand due to introduction of gas can cause class III anomalies in the overpressured zones. For brine sand cases, however, the classes I and II pitfalls persist.

Pre-drill AVO modeling taking into account overpressure can help to reduce the risk of drilling anomalies associated to non-pay zones.

Acknowledgments

We would like to thank PETROBRAS for the permission to publish this work.

References

Lindsay, R. and Towner, B., 2001, Pore pressure influence on rock property and reflectivity modeling, The Leading Edge.

Carcione, J. M. and Gangi, A. F., 2000, Gas generation and overpressure: Effects on seismic attributes, Geophysics, vol 65, n. 6, p.1769-1779.

Rutherford, R. S., **and Williams**, R. H., 1989, Amplitude-versus-offset variation in gas sands: Geophysics, vol 54, p. 680-688.

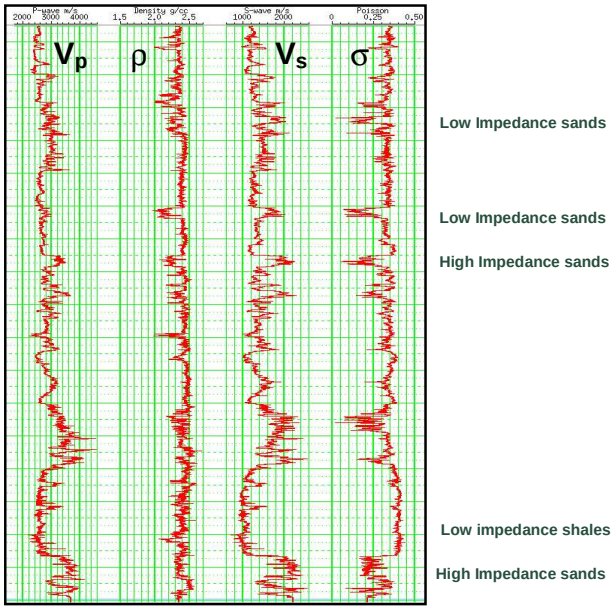

Figure 1 – P-wave velocity, Densitiy (ρ), S-wave velocity and Poisson (σ) logs showing low and high impedance sands. Low impedance sands are predominantly class III reservoirs while high impedance sands are predominantly class II.

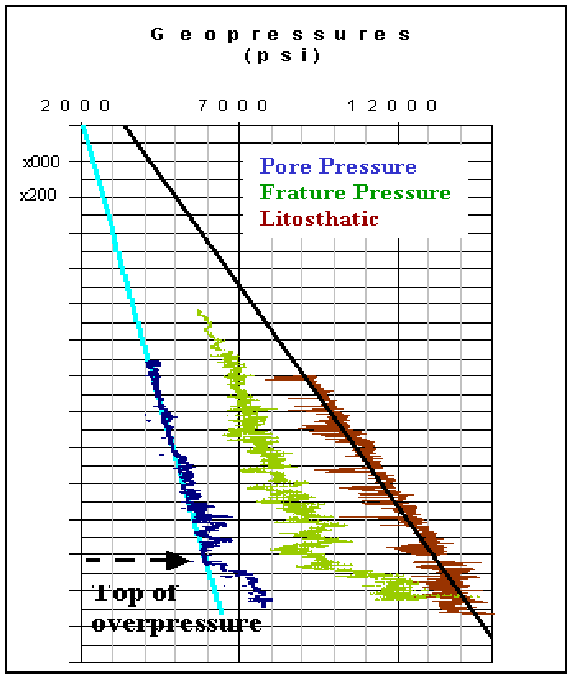

Figure 3 – Geopressure profile.

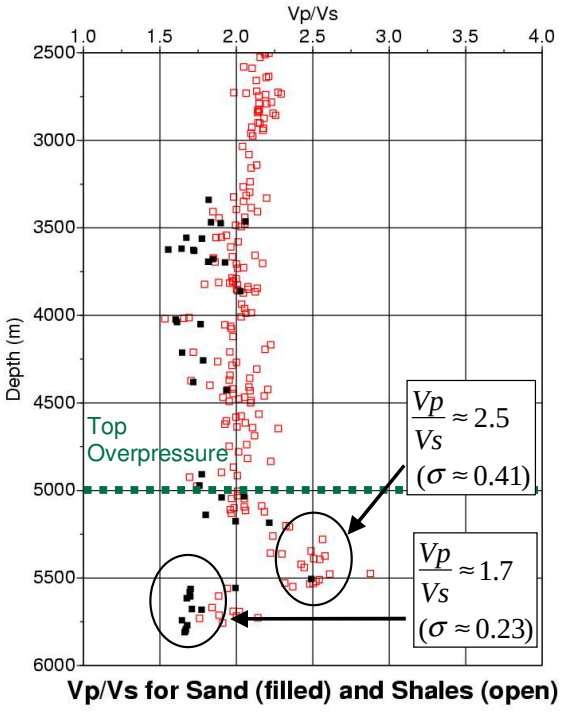

Figure 2 – Vp/Vs ratio for sands (black squares) and shales (open squares). Notice the strong increase in the Poisson's ratio of shales below 5000 m.

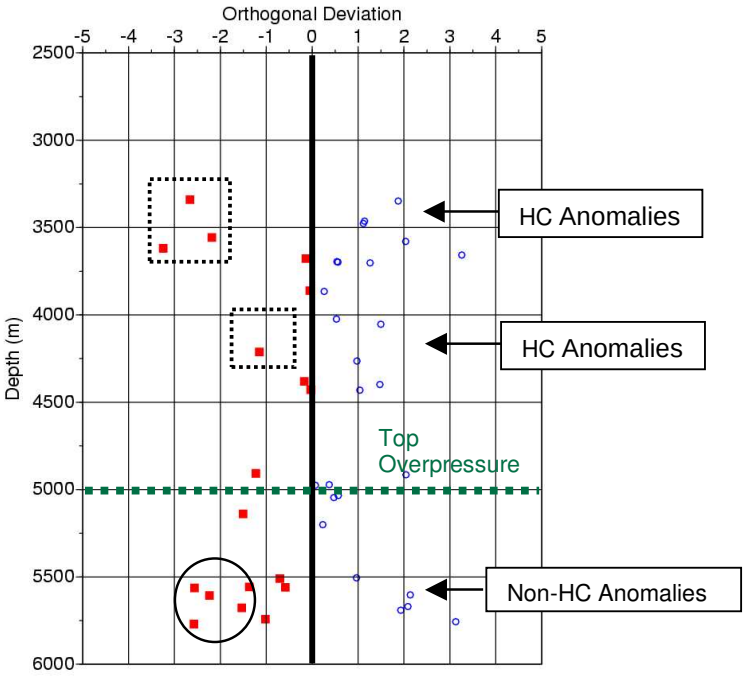

Figure 4 – Orthogonal deviation from AVO background trend. Notice the hydrocarbon related anomalies (dotted squares) and the false AVO anomalies below the top of the overpressure zone (solid circle).

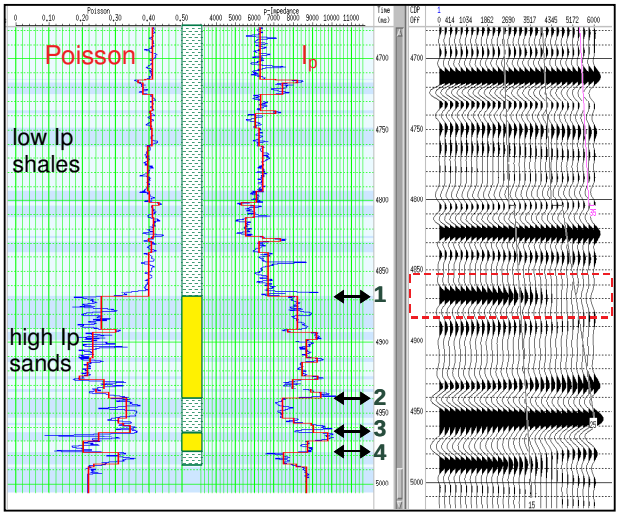

Figure 5 – Poisson´s ratio, P-wave impedance profile and synthetic seismogram highlighting the class II anomaly caused in the contact between overpressured shale and high impedance sand (event 1).

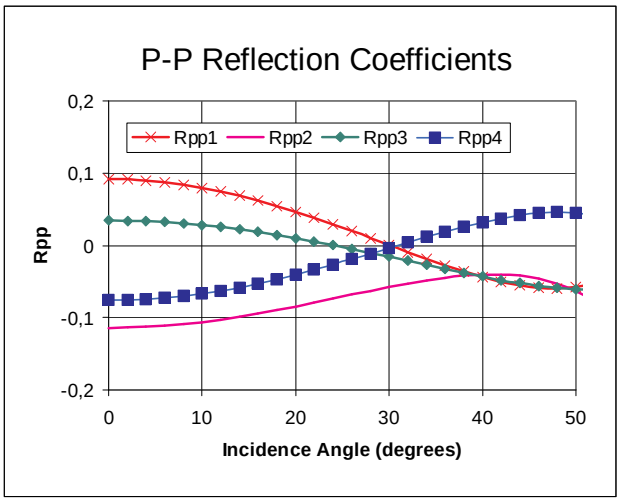

Figure 6 – Reflection coefficient responses for overpressured shale / brine sand (1 and 3), brine sand / overpressured shale (2 and 4) interfaces.

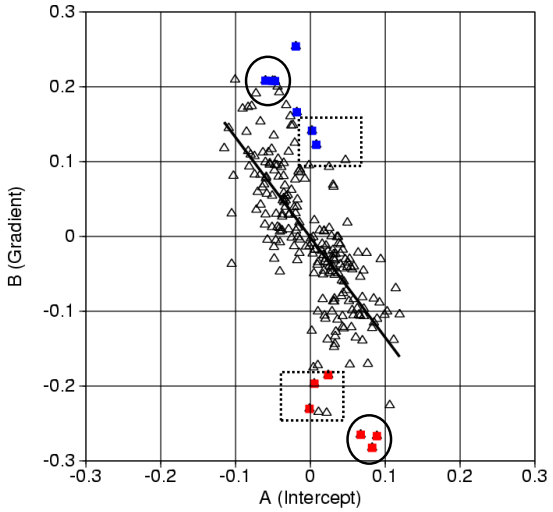

Figure 7 – AVO crossplot for depth interval including the hydrocarbon related class II AVO anomalies (dotted squares) and the deep AVO anomaly promoted by pore pressure (solid circles). Anomalies indicated below the trend correspond to shale/sand interfaces.

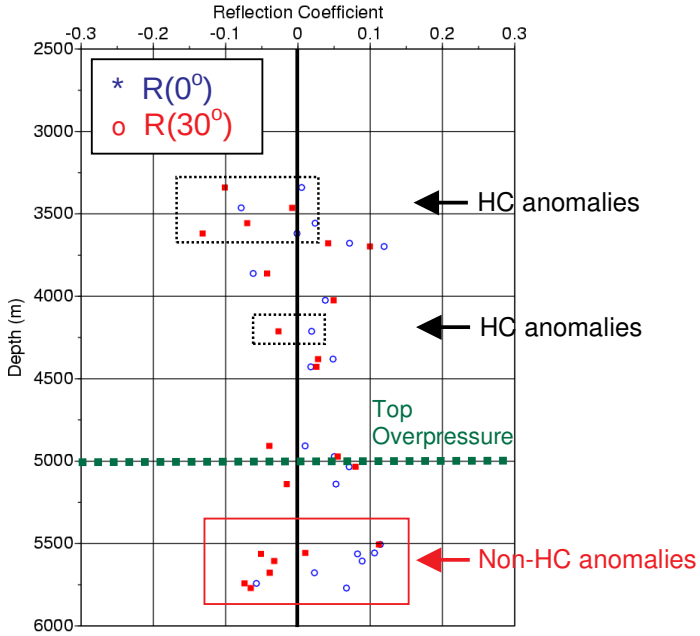

Figure 8 – Reflection coefficients for near (normal incidence) and far (30 degrees incidence) stacks as a function of effective pressure for shale/sand interfaces. The non-hydrocarbon anomalies are indicated by a solid rectangle in the lower part of the figure. Polarity changes indicate class II AVO responses.